Fully correlated study of ${}^{6}_{\Lambda\Lambda}$He hypernucleus including ΛN space-exchange correlations

A. A. Usmani* and Z. Hasan†
Department of Physics, Aligarh Muslim University, Aligarh 202 002, India
(Received 27 November 2005; published 15 September 2006)

We present a fully correlated study of the six-body ${}^{6}_{\Lambda\Lambda}$He hypernucleus. The wave function involves all relevant dynamic correlations as well as the space-exchange correlation (SEC). Calculations for energy breakdown, $\Lambda\Lambda$-separation energy, nuclear core polarization, and point proton radius have been performed. The baryon density profiles have also been calculated. Effect of SEC on all these physical observables is found to be significant. The findings suggest that a study ignoring SEC would be deficient.

DOI: 10.1103/PhysRevC.74.034320 PACS number(s): 21.80.+a, 21.10.Pc

I. INTRODUCTION

The strangeness degree of freedom induces subtle distortions to the properties and symmetries of a bound nucleus. A study of great importance would be to show how this would affect the behavior of the nuclear system with different quanta of strangeness. Besides a large number of single-Λ hypernuclei, we have well-established double-Λ hypernuclear species (${}^{6}_{\Lambda\Lambda}$He, ${}^{10}_{\Lambda\Lambda}$Be, and ${}^{14}_{\Lambda\Lambda}$C) [1–6] to study in detail. Fortunately, experimental data for ${}^{6}_{\Lambda\Lambda}$He ($S=-2$) and ${}^{5}_{\Lambda}$He ($S=-1$) bound with the same core nucleus ^{4}He ($S=0$) are available with reasonable statistics for a successful theoretical estimate. Observation of the ${}^{6}_{\Lambda\Lambda}$He event in the Japanese high energy accelerator research organization (KEK) hybrid experiment [1] E373, called the NAGARA event, and evidence [2] for the bound ${}^{4}_{\Lambda\Lambda}$H ($I=0$, $J=1^{+}$) observed through the (K^{-}, K^{+}) reaction on the ^{9}Be target in the Brookhaven alternating-gradient synchrotron experiment E906 have given fresh impetus to the field of hypernuclei in the $S=-2$ sector on both theoretical and experimental fronts. We find fast advancement on the theoretical front. Recent appearances of many cluster model analyses [7–11] using the Faddeev-Yakubovsky (FY) method have led to notable advancement of the subject. However, while describing the experimental data, an inconsistency linked with the de-excitation of ${}^{10}_{\Lambda\Lambda}$Be* and ${}^{9}_{\Lambda}$Be* through an unobserved γ ray in the detection process also appears, as discussed at length in the variational Monte Carlo (VMC) study of ${}^{6}_{\Lambda\Lambda}$He [12]. This study [12] itself is far from being realistic as it involves only central potentials and correlations. An improved VMC study [13] has also appeared, but it ignores the ΛN space-exchange correlation (SEC) in the wave function (WF). It is evident from recent work [14] on the ${}^{5}_{\Lambda}$He that a study ignoring SEC would be misleading as it significantly affects every physical observable. The effect is expected to be more evident in ${}^{6}_{\Lambda\Lambda}$He hypernucleus because of the presence of a pair of Λ hyperons. Other studies that include the SEC are the FY calculations of ${}^{4}_{\Lambda}$H and ${}^{4}_{\Lambda}$He by Nogga *et al.* [15], yet to be extended to five- and six-body hypernuclei, and the variational calculations of s-shell single hypernuclei by Nemura *et al.* [16], which explicitly include the Σ channel at the two-body level. The SEC is naturally built into these formalisms; therefore, its effect cannot be deduced directly as done for ${}^{5}_{\Lambda}$He in Ref. [14] and for ${}^{6}_{\Lambda\Lambda}$He in this study.

The SEC also implicates various subtle issues, such as the physical existence of a bound ${}^{4}_{\Lambda\Lambda}$H, SU(3) symmetry breaking of baryon-baryon (BB) potential and the question whether we can successfully reproduce the hypernuclear energy spectra using realistic BB and three-baryon ($3B$) interactions without including the underlying quantum chromodynamics (QCD). Thus, a fully correlated study of the ${}^{6}_{\Lambda\Lambda}$He hypernucleus presented in this paper is an important contribution.

II. HAMILTONIAN AND WAVE FUNCTION

A full nonrelativistic Hamiltonian ($H_{\Lambda\Lambda}$) of the A-baryon double-Λ hypernucleus is written as

$$H = H_{\rm NC} + H_{\Lambda_1} + H_{\Lambda_2} + v_{\Lambda_1\Lambda_2}, \tag{1}$$

where $H_{\rm NC}$ is the nonstrange nuclear core Hamiltonian

$$H_{\rm NC} = T_{\rm NC} + \sum_{i<j}^{A-2} v_{ij} + \sum_{i<j<k}^{A-2} V_{ijk}, \tag{2}$$

H_{Λ_n} is the Hamiltonian arising due to an individual Λ_n

$$H_{\Lambda_n} = T_{\Lambda_n} + \sum_{i}^{A-2} v_{\Lambda_n i} + \sum_{i<j}^{A-2} V_{\Lambda_n ij}, \tag{3}$$

and $v_{\Lambda_1\Lambda_2}$ is the $\Lambda\Lambda$ potential. Obviously, $H_{\rm NC}+H_{\Lambda_n}$ is Hamiltonian for the $(A-1)$ baryon single-Λ hypernucleus.

The basic ingredients in these Hamiltonians are BB and $3B$ forces. For the $S=-2$ sector, we use phase equivalent Nijmegen $\Lambda\Lambda$ potentials represented by three range Gaussian functions [8,11,17,18]

$$v_{\Lambda\Lambda}(r) = v_1 \exp\left(-\frac{r^2}{\beta_1^2}\right) + \gamma v_2 \exp\left(-\frac{r^2}{\beta_2^2}\right) + v_3 \exp\left(-\frac{r^2}{\beta_3^2}\right). \tag{4}$$

Here range parameters β_i and strength parameters v_i are taken from Ref. [8]. The dimensionless quantity γ distinguishes

*Also at the Inter University Centre for Astronomy and Astrophysics (IUCAA), Ganeshkhind, Pune-411 007, India; Electronic address: anisul@iucaa.ernet.in
†Electronic address: zafar_amu@rediffmail.com

among various Nijmegen potential models. For example, NSC97e, ND, and NEC00 are represented by $\gamma = 0.5463$, $\gamma = 1.0$, and $\gamma = 1.2044$, respectively. For the $S = -1$ sector, we use the charge symmetric ΛN potential [19,20] written as

$$v_{\Lambda N}(r) = v_0(r)(1 - \varepsilon + \varepsilon P_x) + (v_\sigma/4)T_\pi^2(r)\boldsymbol{\sigma}_\Lambda \cdot \boldsymbol{\sigma}_N, \quad (5)$$

with

$$v_0(r) = v_c(r) - \overline{v}T_\pi^2(r). \quad (6)$$

Here,

$$v_c(r) = \frac{W_c}{1 + \exp\left(\frac{r-R}{ar}\right)} \quad (7)$$

is the Saxon-Woods repulsive potential, $T_\pi(r)$ is the one-pion exchange tensor potential

$$T_\pi(r) = \left(1 + \frac{3}{\mu r} + \frac{3}{(\mu r)^2}\right)\frac{\exp(-\mu r)}{\mu r}\left[1 - \exp(-cr^2)\right]^2, \quad (8)$$

$\mu = 0.7$ fm^{-1}is the pion mass, $c = 2.0$ fm^{-2} is the cutoff parameter, ε is the space-exchange strength, and P_x is the Majorana space-exchange operator. The $\overline{v} = (v_s + 3v_t)/4$ and $v_\sigma = v_s - v_t$ are, respectively, the spin-average and spin-dependent strengths, with $v_{s(t)}$ the singlet(triplet) state depths. The $\overline{v} \approx 6.15(5)$ MeV is found consistent with low energy Λp scattering data [21]. For the $S = 0$ nonstrange sector, we use the realistic two-nucleon (NN) Argonne v_{18} potential [22].

In addition to these, we use the three-nucleon (NNN) Urbana model-IX potential [23,24] and the three-baryon (ΛNN) potential [21,25,26]. The ΛNN potential ($V_{\Lambda NN}$) is represented by two terms

$$V_{\Lambda NN} = V_{\Lambda NN}^D + V_{\Lambda NN}^{2\pi}. \quad (9)$$

Here, $V_{\Lambda NN}^D$ is a dispersive force, suggested by the suppression mechanism due to ΛN-ΣN coupling [27–30], which is written with explicit spin dependence as [21]

$$V_{\Lambda ij}^D = W^D T_\pi^2(r_{\Lambda i})T_\pi^2(r_{\Lambda j})[1 + \boldsymbol{\sigma}_\Lambda \cdot (\boldsymbol{\sigma}_i + \boldsymbol{\sigma}_j)/6]. \quad (10)$$

The $V_{\Lambda NN}^{2\pi}$ is a sum of two terms due to p- and s-wave $\pi - N$ scatterings, which are written as

$$V_{\Lambda ij}^P = -(C^P/6)(\boldsymbol{\tau}_i \cdot \boldsymbol{\tau}_j)\{X_{i\Lambda}, X_{\Lambda j}\}, \quad (11)$$

$$V_{\Lambda ij}^S = C^S Z(r_{i\Lambda})Z(r_{j\Lambda})\boldsymbol{\sigma}_i \cdot \hat{\mathbf{r}}_{i\Lambda}\boldsymbol{\sigma}_j \cdot \hat{\mathbf{r}}_{j\Lambda}\boldsymbol{\tau}_i \cdot \boldsymbol{\tau}_j, \quad (12)$$

with

$$X_{\Lambda i} = (\boldsymbol{\sigma}_\Lambda \cdot \boldsymbol{\sigma}_i)Y_\pi(r_{\Lambda i}) + S_{\Lambda i}T_\pi(r_{\Lambda i}), \quad (13)$$

and

$$Z(r) = \frac{\mu r}{3}[Y_\pi(r) - T_\pi(r)]. \quad (14)$$

Here, W^D, C^P, and C^S are strengths, $S_{\Lambda i} = 3(\boldsymbol{\sigma}_\Lambda \cdot \hat{\mathbf{r}}_{\Lambda i})(\boldsymbol{\sigma}_i \cdot \hat{\mathbf{r}}_{\Lambda i}) - \boldsymbol{\sigma}_\Lambda \cdot \boldsymbol{\sigma}_i$ is the tensor operator, and Y_π is the Yukawa function

$$Y_\pi(r) = \frac{\exp(-\mu r)}{\mu r}[1 - \exp(-cr^2)]. \quad (15)$$

We use the fully correlated WF by Usmani [14] that includes all relevant dynamic correlations along with the SEC. For the A-baryon s-shell hypernucleus with l number of Λ hyperons and $A - l$ number of nucleons, it reads as

$$|\Psi\rangle = \left[1 + U^3 + \sum_{i<j}^{A-l} U_{ij}^{LS}\right]\left[\prod_{j=1}^{A-l}\left(1 + u_{\Lambda j}^\sigma\right)\right] \times \left[S\prod_{i<j}^{A-l}\left(1 + U_{ij}\right)\right]\Psi_J + \frac{\eta}{\Lambda_p}\sum_{\lambda=1}^{l}\sum_{n=1}^{A-l}[1 + U^3] \times \left[S\prod_{i<j}^{A-l}(1 + U_{ij})\right]\Psi_J u_{\lambda n}^x P_x.$$

Here,

$$U^3 = 1 + \sum_{\lambda=1}^{l}\sum_{j<k}^{A-l} U_{\lambda jk} + \sum_{i<j<k}^{A-l}\left(U_{ijk} + U_{ijk}^{TNI}\right) \quad (16)$$

and

$$\Psi_J = \left[\prod_{\lambda=1}^{l}\prod_{j<k}^{A-l} f_{\lambda jk}^c\right]\left[\prod_{\lambda=1}^{l}\prod_{j=1}^{A-l} f_{\Lambda j}^c\right] \left[\prod_{\lambda=1}^{l-1} f_{\Lambda\lambda}^c\right]\left[\prod_{i<j<k}^{A-l} f_{ijk}^c\right]\left[\prod_{i<j}^{A-l} f_{ij}^c\right]\chi_\Lambda^\sigma \Psi_{JT}. \quad (17)$$

Except for the $\Lambda\Lambda$ correlation function $f_{\Lambda\Lambda}^c$, all other correlation functions are defined in Ref. [14]. Implementation of the P_x operation between Λ and nucleon on a ΛN pair is also discussed therein. The $f_{\Lambda\Lambda}^c$ is obtained by solving the Schrödinger equation with phase equivalent Nijmegen potential $v_{\Lambda\Lambda}$ along with an auxiliary potential involving many asymptotic parameters originally defined in Ref. [21]. The $\chi_\Lambda^\sigma = \mathcal{A}|\downarrow \Lambda \uparrow \Lambda\rangle$ is the antisymmetric spin wave function of two Λ hyperons coupled to total angular momentum zero.

III. ENERGY CALCULATION

The important energies that we wish to calculate are defined as follows:

(i) the separation energy of two Λ hyperons from the core nucleus of ${}^{\ 6}_{\Lambda\Lambda}$He,

$$B_{\Lambda\Lambda} = \frac{\langle\Psi_{A-2}|H_{\rm NC}|\Psi_{A-2}\rangle}{\langle\Psi_{A-2}|\Psi_{A-2}\rangle} - \frac{\langle\Psi_A|H|\Psi_A\rangle}{\langle\Psi_A|\Psi_A\rangle}, \quad (18)$$

(ii) the separation energy of a single Λ from the same core nucleus of ${}^{\ 5}_{\Lambda}$He,

$$B_\Lambda = \frac{\langle\Psi_{A-2}|H_{\rm NC}|\Psi_{A-2}\rangle}{\langle\Psi_{A-2}|\Psi_{A-2}\rangle} - \frac{\langle\Psi_{A-1}|H_{\rm NC} + H_{\Lambda_1}|\Psi_{A-1}\rangle}{\langle\Psi_{A-1}|\Psi_{A-1}\rangle}, \quad (19)$$

(iii) the incremental energy

$$\Delta B_{\Lambda\Lambda} = B_{\Lambda\Lambda} - 2B_\Lambda, \quad (20)$$

and (iv) the rearrangement energy E_R also known as the nuclear core polarization (NCP), which is the difference of the internal energy of the $(A - l)$ subsystem and the energy of

TABLE I. ΛN potential strengths in units of MeV.

	v_s	v_t	$\overline{v} = (v_s + 3v_t)/4$	$v_\sigma = v_s - v_t$
$\overline{v}1$	6.33	6.09	6.15	0.24
$\overline{v}2$	6.28	6.04	6.10	0.24
$\overline{v}3$	6.23	5.99	6.05	0.24

an identical isolated bound nucleus, that is,

$$\text{NCP} = E_R = E^{\text{int}}_{\text{NC}} - E_{^4\text{He}}, \tag{21}$$

where

$$E^{\text{int}}_{\text{NC}} = T^{\text{int}}_{\text{NC}} + V_{\text{NC}}, \tag{22}$$

with

$$T^{\text{int}}_{\text{NC}} = \sum_{i=1}^{A-l} \frac{p_i^2}{2m_N} - \frac{\left(\sum_{i=1}^{A-l} p_i\right)^2}{2(A-l)m_N} \equiv T_{\text{NC}} - T^{\text{c.m.}}_{\text{NC}}. \tag{23}$$

Here, $T^{\text{c.m.}}_{\text{NC}}$ is the kinetic energy due to c.m. motion of the subsystem around the c.m. of the hypernucleus.

The variational energy, $E_{^5_\Lambda\text{He}} = \frac{\langle\Psi_{A-1}|H_{\text{NC}}+H_{\Lambda_1}|\Psi_{A-1}\rangle}{\langle\Psi_{A-1}|\Psi_{A-1}\rangle}$, of ${}^5_\Lambda$He hypernucleus and other results related to it are borrowed from Ref. [14]. These are obtained using the Hamiltonian, $H_{\text{NC}} + H_{\Lambda_1}$, and the WF as given by Eq. (16) but with $l = 1$, thereby discluding the correlation functions that arise because of the presence of the second Λ hyperon. The basic ingredients used herein for the $S = -1$ sector are the two- and three-baryon potential strengths as reported in Ref. [14]. We use three different sets of spin-average strength $\overline{v}$ and a constant spin-dependent strength v_σ, as in Table I and referred to as $\overline{v}1$, $\overline{v}2$, and $\overline{v}3$. With each set, three values of space-exchange strength ε=0.1, 0.2, and 0.3 are chosen, which are in the range 0.1–0.38 [27]. For the two-pion exchange potential strengths, we take $W^S = 1.5$ and $W^P = 0.75$ MeV. The repulsive strength W^D is then adjusted to reproduce the experimental Λ-separation energy [$B^{\text{exp}}_\Lambda = 3.12(2)$ MeV]. For the $\varepsilon = 0.1$ and with $\overline{v}1$, $\overline{v}2$, and $\overline{v}3$, the value of W^D is found to be 0.0193, 0.0158, and 0.0115 MeV, respectively. We also use the result, $\partial W^D/\partial\varepsilon \approx -0.017$ MeV, as reported in the above reference, to reproduce the B^{exp}_Λ for any value of ε.

Using these potential strengths in the $S = -1$ sector along with the Nijmegen ND model $\Lambda\Lambda$ potential in the $S = -2$ sector, we perform calculations for variational energy $E_{^{6}_{\Lambda\Lambda}\text{He}} = \frac{\langle\Psi_A|H|\Psi_A\rangle}{\langle\Psi_A|\Psi_A\rangle}$, of ${}^{6}_{\Lambda\Lambda}$He. First of all, we use the full WF including SEC. We observe that the WF needs to be retuned afresh with any change in the potential strengths. The optimal correlation functions so obtained are plotted in Fig. 1, where $f^c_{\Lambda N}(r)$, $u^x_{\Lambda N}(r)$, and $f^c_{\Lambda\Lambda}(r)$ are represented by solid, dashed, and long-dashed lines, respectively. We then switch off SEC in the WF, which is equivalent to ignoring the second term in the WF, and then retune the variational parameters for an independent energy calculation. Optimal correlation functions, $f^c_{\Lambda N}(r)$ and $f^c_{\Lambda\Lambda}(r)$, for this case as well, are reported in Fig. 1. In the case of no SEC, unlike that for ${}^5_\Lambda$He, the WF is not found constant for ${}^{6}_{\Lambda\Lambda}$He with the variation of ε which offsets few parameters of the WF. Thus for both the cases with and without SEC, should a change be made in the ε, the WF is tuned afresh.

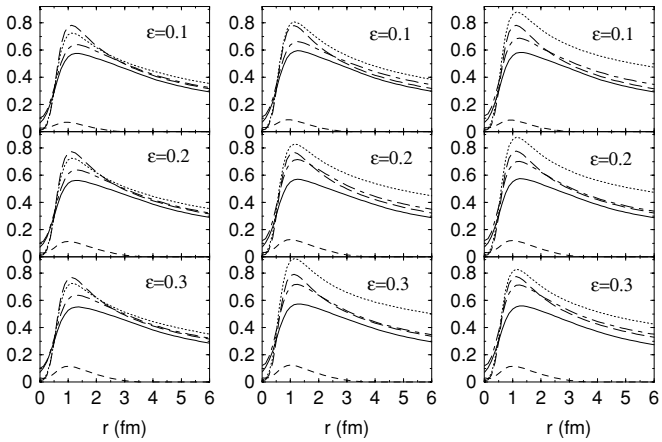

FIG. 1. Solid, dashed, and long-dashed lines represent $f^c_{\Lambda N}(r)$, $u^x_{\Lambda N}(r)$, and $f^c_{\Lambda\Lambda}(r)$ with SEC. Chain and dotted lines represent $f^c_{\Lambda N}(r)$ and $f^c_{\Lambda\Lambda}(r)$ with no SEC. Left, middle, and right columns represent $\overline{v}1$, $\overline{v}2$, and $\overline{v}3$, respectively.

IV. RESULTS AND DISCUSSION

The energy breakdowns are reported with and without SEC in Tables II, III, and IV for the three sets of strengths $\overline{v}1$, $\overline{v}2$, and $\overline{v}3$, respectively. In each table, results for $\varepsilon = 0.1$, 0.2, and 0.3 are presented. Comparison of the results show a significant SEC effect in every piece of energy breakdown. The SEC effect on the total energy of the hypernucleus or on $B_{\Lambda\Lambda}$ is lowest for the lowest value of ε. However, its effect is always found greater than 0.5 MeV, which is not small. The energies are found sensitive to SEC and hence to ε. They are also sensitive to other operatorial correlations. The detailed analysis of the energy breakdown is presented in the following paragraphs. Discussion also follows on the SEC effects on the nuclear core polarization, density profiles, and point proton radius.

The average value of P_x, $\langle P_x\rangle = \langle v_0(r)\varepsilon P_x\rangle/\langle v_0(r)\varepsilon\rangle$, may directly be deduced from the data in Tables II–IV in the case of no SEC, which is about 0.87(1) for all the choices of $\overline{v}$. With SEC, however, WF involves another P_x operator, which alters the value of $\langle P_x\rangle$, but slightly. As a result, it is always less than 1.0 for both choices of the WF, that is, with and without SEC. Hence, the sum of the expectation values of central and space-exchange parts of the ΛN potential, $\langle v_0(r)(1-\varepsilon)\rangle + \langle v_0(r)\varepsilon P_x\rangle$ (which is a negative quantity), would decrease linearly with decreasing ε, provided WF remains constant. This is almost all of the $v_{\lambda i}$ potential, whose spin part $\langle(\frac{1}{4})v_\sigma T^2_\pi(r)\boldsymbol{\sigma}_\lambda\cdot\boldsymbol{\sigma}_i\rangle$ is very weak. We observe that in the case of no SEC and only for $\overline{v}1$, WF is invariant with the variation of ε. As a consequence, a linear relationship $\partial v_{\lambda i}/\partial\varepsilon \approx 5.0$ MeV is observed (Table II). However, for all other cases, with or without SEC, WF changes with the variation of ε. Hence, the above relationship is not seen in these cases. The central correlation $f^c_{\Lambda N}$ is a solution of the potential $v_{\lambda i}$. Therefore, the spin-averaged strength $\overline{v}$ that explicitly appears in Eq. [(6)] plays a role. It may lead to a significant change in the correlation function even without SEC, which we do observe for $\overline{v}2$ and $\overline{v}3$. The SEC modifies the WF and hence the density profiles. Its sensitivity with ε has already

TABLE II. Energy breakdown of the ${}^{6}_{\Lambda\Lambda}$He for $\overline{v}1$ ($\overline{v} = 6.15$ MeV, $v_\sigma = 0.24$ MeV). Except for ε, all quantities are in units of MeV. Subscripts i, j, and k refer to nucleons, and λ refers to Λ hyperons.

	$\varepsilon = 0.1$			$\varepsilon = 0.2$			$\varepsilon = 0.3$		
	(SEC) A	(No SEC) B	A-B	(SEC) C	(No SEC) D	C-D	(SEC) E	(No SEC) F	E-F
$T_\Lambda = T_{\Lambda_1} + T_{\Lambda_2}$	22.51(6)	21.08(6)	1.43(8)	21.73(6)	21.08(6)	0.65(8)	21.62(6)	21.08(6)	0.54(8)
$v_0(r)(1-\varepsilon)$	−33.67(8)	−32.65(8)	−1.02(11)	−29.31(7)	−29.02(7)	−0.29(10)	−25.38(6)	−25.39(6)	0.01(8)
$v_0(r)\varepsilon P_x$	−3.24(1)	−3.14(1)	−0.10(1)	−6.37(2)	−6.27(2)	−0.10(3)	−9.48(3)	−9.41(3)	−0.07(4)
$(\frac{1}{4})v_\sigma T_\pi^2(r)\boldsymbol{\sigma}_\lambda \cdot \boldsymbol{\sigma}_i$	0.06(0)	0.046(0)	0.014(0)	0.06(0)	0.046(0)	0.014(0)	0.05(0)	0.046(0)	0.004(0)
$v_{\lambda i}$	−36.84(9)	−35.74(8)	−1.10(12)	−35.62(9)	−35.25(8)	−0.37(12)	−34.83(9)	−34.75(8)	−0.08(12)
$v_{\Lambda\Lambda} = v_{\Lambda_1\Lambda_2}(\gamma = 1.0)$	−5.99(5)	−4.65(5)	−1.34(7)	−5.51(5)	−4.65(5)	−0.86(7)	−5.49(5)	−4.65(5)	−0.84(7)
$V^D_{\lambda ij}$	6.08(2)	5.65(2)	0.43(3)	5.61(2)	5.15(2)	0.46(3)	4.99(2)	4.65(2)	0.34(3)
$V^P_{\lambda ij}$	−4.81(2)	−5.71(2)	0.90(3)	−4.97(2)	−5.71(2)	0.74(3)	−4.75(2)	−5.71(2)	0.96(3)
$V^S_{\lambda ij}$	−0.05(0)	−0.049(0)	−0.001(0)	−0.01(0)	−0.049(0)	0.039(0)	−0.05(0)	−0.049(0)	−0.001(0)
$V^{2\pi}_{\lambda ij} = V^P_{\lambda ij} + V^S_{\lambda ij}$	−4.86(2)	−5.75(2)	0.89(3)	−4.97(2)	−5.75(2)	0.78(3)	−4.80(2)	−5.75(2)	0.95(3)
$V_{\lambda ij} = V^D_{\lambda ij} + V^{2\pi}_{\lambda ij}$	1.22(2)	−0.11(1)	1.33(2)	0.64(2)	−0.60(2)	1.24(3)	0.19(2)	−1.10(2)	1.29(3)
$V_\Lambda = v_{\lambda i} + v_{\lambda\lambda} + V_{\lambda ij}$	−41.52(9)	−40.50(8)	−1.02(12)	−40.50(9)	−40.50(8)	0.00(12)	−40.13(9)	−40.50(8)	0.37(12)
$E_\Lambda = T_\Lambda + V_\Lambda$	−19.01(5)	−19.42(5)	0.41(7)	−18.77(5)	−19.42(5)	0.65(7)	−18.51(5)	−19.42(5)	0.91(7)
$T_{\rm NC}$	121.05(16)	119.32(15)	1.73(22)	119.94(15)	119.32(15)	0.62(21)	119.91(15)	119.32(15)	0.59(21)
v_{NN}	−131.75(14)	−129.43(14)	−2.32(20)	−130.95(14)	−129.43(14)	−1.52(20)	−131.04(14)	−129.43(14)	−1.61(20)
V_{NNN}	−5.58(2)	−5.18(2)	−0.40(3)	−5.52(2)	−5.18(2)	−0.34(3)	−5.63(2)	−5.18(2)	−0.45(3)
$V_{\rm NC} = v_{ij} + V_{ijk}$	−137.33(15)	−134.61(15)	−2.72(21)	−136.47(15)	−134.61(14)	−1.86(21)	−136.67(15)	−134.61(14)	−2.06(21)
$E_{\rm NC} = T_{\rm NC} + V_{\rm NC}$	−16.29(6)	−15.29(4)	−1.00(7)	−16.53(6)	−15.29(4)	−1.24(7)	−16.76(6)	−15.29(4)	−1.47(7)
$E_{{}^{6}_{\Lambda\Lambda}{\rm He}} = E_\Lambda + E_{\rm NC}$	−35.30(5)	−34.72(4)	−0.58(6)	−35.30(5)	−34.72(4)	−0.58(6)	−35.27(5)	−34.72(4)	−0.55(6)
$B_{\Lambda\Lambda}$	7.57(5)	6.99(4)	0.58(6)	7.57(5)	6.99(4)	0.58(6)	7.54(5)	6.99(4)	0.55(6)
$\Delta B_{\Lambda\Lambda}$	1.33(6)	0.75(4)	0.58(7)	1.33(6)	0.75(4)	0.58(7)	1.30(6)	0.75(4)	0.55(7)

TABLE III. Energy breakdown of the ${}^{6}_{\Lambda\Lambda}$He for $\overline{v}2$ ($\overline{v} = 6.10$ MeV, $v_\sigma = 0.24$ MeV). Except for ε, all quantities are in units of MeV. Subscripts i, j, and k refer to nucleons, and λ refers to Λ hyperons.

	$\varepsilon = 0.1$			$\varepsilon = 0.2$			$\varepsilon = 0.3$		
	(SEC) A	(No SEC) B	A-B	(SEC) C	(No SEC) D	C-D	(SEC) E	(No SEC) F	E-F
$T_\Lambda = T_{\Lambda_1} + T_{\Lambda_2}$	23.38(7)	20.20(6)	3.18(9)	22.94(6)	22.01(6)	0.93(8)	22.63(6)	22.30(7)	0.33(9)
$v_0(r)(1-\varepsilon)$	−33.87(8)	−30.74(8)	−3.13(11)	−29.64(8)	−30.32(7)	0.68(11)	−26.03(7)	−26.71(7)	0.68(10)
$v_0(r)\varepsilon P_x$	−3.28(1)	−2.96(1)	−0.32(1)	−6.46(2)	−6.58(2)	0.12(3)	−9.75(3)	−9.95(3)	0.20(4)
$(\frac{1}{4})v_\sigma T_\pi^2(r)\boldsymbol{\sigma}_\lambda \cdot \boldsymbol{\sigma}_i$	0.08(0)	0.078(0)	0.002(0)	0.02(0)	0.038(0)	−0.018(0)	0.03(0)	0.029(0)	0.001(0)
$v_{\lambda i}$	−37.07(9)	−33.62(9)	−3.45(13)	−36.07(9)	−36.86(9)	0.79(13)	−35.76(9)	−36.63(9)	0.87(13)
$v_{\Lambda\Lambda} = v_{\Lambda_1\Lambda_2}(\gamma = 1.0)$	−6.01(5)	−4.83(4)	−1.18(6)	−5.74(5)	−4.49(5)	−1.25(7)	−5.38(5)	−4.64(5)	−0.74(7)
$V^D_{\lambda ij}$	5.61(2)	5.09(2)	0.52(3)	5.03(2)	5.38(2)	−0.35(3)	4.33(2)	4.88(2)	−0.55(3)
$V^P_{\lambda ij}$	−5.39(2)	−4.97(2)	−0.42(3)	−6.00(2)	−6.08(2)	0.08(3)	−5.68(2)	−6.43(3)	0.75(4)
$V^S_{\lambda ij}$	−0.01(0)	−0.049(0)	0.039(0)	−0.01(0)	−0.044(0)	0.034(0)	−0.04(0)	−0.007(0)	−0.033(0)
$V^{2\pi}_{\lambda ij} = V^P_{\lambda ij} + V^S_{\lambda ij}$	−5.40(2)	−5.02(2)	−0.38(3)	−6.01(2)	−6.13(2)	0.12(3)	−5.72(2)	−6.44(2)	0.72(3)
$V_{\lambda ij} = V^D_{\lambda ij} + V^{2\pi}_{\lambda ij}$	0.21(2)	0.06(2)	0.15(3)	−0.99(2)	−0.75(2)	−0.24(3)	−1.39(2)	−1.56(2)	0.17(3)
$V_\Lambda = v_{\lambda i} + v_{\lambda\lambda} + V_{\lambda ij}$	−42.88(9)	−38.39(8)	−4.49(12)	−42.80(9)	−42.09(8)	−0.71(12)	−42.53(9)	−42.84(8)	0.31(12)
$E_\Lambda = T_\Lambda + V_\Lambda$	−19.05(5)	−18.19(5)	−0.86(7)	−19.86(5)	−20.09(5)	0.23(7)	−19.91(5)	−20.53(5)	0.62(7)
$T_{\rm NC}$	121.38(23)	119.49(15)	1.89(27)	121.31(22)	126.21(24)	−4.90(33)	121.88(22)	126.83(24)	−4.95(33)
v_{NN}	−131.48(19)	−130.65(14)	−0.83(24)	−131.41(19)	−134.95(20)	3.54(28)	−132.06(19)	−135.22(20)	3.16(28)
V_{NNN}	−5.57(2)	−5.29(2)	−0.28(3)	−5.52(2)	−5.63(2)	0.11(3)	−5.61(2)	−5.71(2)	0.10(3)
$V_{\rm NC} = v_{ij} + V_{ijk}$	−137.16(15)	−135.95(15)	−1.21(21)	−136.92(15)	−140.58(15)	3.66(21)	−137.67(15)	−140.93(15)	3.26(21)
$E_{\rm NC} = T_{\rm NC} + V_{\rm NC}$	−15.67(7)	−16.46(6)	0.79(9)	−15.61(7)	−14.45(7)	−1.16(10)	−15.79(7)	−14.10(6)	−1.69(9)
$E_{{}^{6}_{\Lambda\Lambda}{\rm He}} = E_\Lambda + E_{\rm NC}$	−35.18(5)	−34.65(3)	−0.53(6)	−35.47(5)	−34.45(3)	−1.02(6)	−35.69(5)	−34.63(3)	−1.06(6)
$B_{\Lambda\Lambda}$	7.45(5)	6.92(4)	0.53(6)	7.74(5)	6.72(4)	1.02(6)	7.96(5)	6.90(4)	1.06(6)
$\Delta B_{\Lambda\Lambda}$	1.21(6)	0.68(4)	0.53(7)	1.50(6)	0.48(4)	1.02(7)	1.72(6)	0.66(4)	1.06(7)

TABLE IV. Energy breakdown of the ${}^{6}_{\Lambda\Lambda}$He for $\overline{v}3$ ($\overline{v} = 6.05$ MeV, $v_\sigma = 0.24$ MeV). Except for ε, all quantities are in units of MeV. Subscripts i, j and k refer to nucleons, and λ refers to Λ hyperons.

	$\varepsilon = 0.1$			$\varepsilon = 0.2$			$\varepsilon = 0.3$		
	(SEC) A	(No SEC) B	A-B	(SEC) C	(No SEC) D	C-D	(SEC) E	(No SEC) F	E-F
$T_\Lambda = T_{\Lambda_1} + T_{\Lambda_2}$	23.12(7)	19.64(6)	3.48(9)	23.39(7)	23.36(6)	0.03(9)	24.32(7)	22.52(6)	1.80(9)
$v_0(r)(1-\varepsilon)$	−31.95(8)	−29.51(8)	−2.44(11)	−29.01(7)	−30.12(8)	1.11(11)	−26.16(7)	−25.17(7)	−0.99(10)
$v_0(r)\varepsilon P_x$	−3.07(1)	−2.83(1)	−0.24(1)	−6.33(2)	−6.53(2)	0.20(3)	−9.73(3)	−9.28(3)	−0.45(4)
$(\frac{1}{4})v_\sigma T_\pi^2(r)\boldsymbol{\sigma}_\lambda \cdot \boldsymbol{\sigma}_i$	0.05(0)	0.052(0)	−0.002(0)	0.16(0)	0.027(0)	0.133(0)	0.03(0)	0.009(0)	0.021(0)
$v_{\lambda i}$	−34.98(9)	−32.29(9)	−2.69(13)	−35.33(9)	−36.65(9)	1.32(13)	−35.87(9)	−34.44(9)	−1.43(13)
$v_{\Lambda\Lambda} = v_{\Lambda_1\Lambda_2}(\gamma = 1.0)$	−6.03(5)	−4.22(4)	−1.81(6)	−5.79(5)	−4.89(5)	−0.90(7)	−6.97(5)	−4.72(4)	−2.25(6)
$V^D_{\lambda ij}$	3.87(2)	3.98(1)	−0.11(2)	3.40(2)	3.99(1)	−0.59(2)	2.83(2)	2.90(1)	−0.07(2)
$V^P_{\lambda ij}$	−4.98(2)	−5.37(2)	0.39(3)	−5.55(2)	−6.88(3)	1.33(4)	−6.09(2)	−7.20(3)	1.11(4)
$V^S_{\lambda ij}$	−0.03(0)	−0.042(0)	0.012(0)	−0.02(0)	−0.036(0)	0.016(0)	−0.04(0)	−0.064(0)	0.024(0)
$V^{2\pi}_{\lambda ij} = V^P_{\lambda ij} + V^S_{\lambda ij}$	−5.00(2)	−5.41(2)	0.41(3)	−5.58(2)	−6.92(3)	1.34(4)	−6.13(2)	−7.27(3)	1.14(4)
$V_{\lambda ij} = V^D_{\lambda ij} + V^{2\pi}_{\lambda ij}$	−1.13(2)	−1.43(2)	0.30(3)	−2.18(2)	−2.93(2)	0.75(3)	−3.31(2)	−4.36(2)	1.05(3)
$V_\Lambda = v_{\lambda i} + v_{\lambda\lambda} + V_{\lambda ij}$	−42.14(9)	−37.93(8)	−4.21(12)	−43.30(9)	−41.54(8)	−1.76(12)	−45.14(9)	−43.53(8)	−1.61(12)
$E_\Lambda = T_\Lambda + V_\Lambda$	−19.02(5)	−18.29(5)	−0.73(7)	−19.91(5)	−21.10(5)	1.19(7)	−20.83(5)	−21.01(5)	0.18(7)
$T_{\rm NC}$	121.87(23)	121.87(15)	0.00(27)	121.53(22)	127.30(25)	−5.77(33)	126.68(23)	128.69(24)	−2.01(33)
v_{NN}	−132.28(19)	−132.43(14)	0.15(24)	−131.49(19)	−135.09(20)	3.60(28)	−135.46(19)	−136.80(20)	1.34(28)
V_{NNN}	−5.62(2)	−5.46(2)	−0.16(3)	−5.49(2)	−5.61(2)	0.12(3)	−5.92(2)	−5.63(2)	−0.29(3)
$V_{\rm NC} = v_{ij} + V_{ijk}$	−137.90(15)	−137.89(15)	−0.01(21)	−136.98(15)	−140.70(15)	3.72(21)	−141.52(15)	−142.43(15)	0.91(21)
$E_{\rm NC} = T_{\rm NC} + V_{\rm NC}$	−16.05(6)	−16.04(7)	−0.01(9)	−15.45(7)	−13.40(7)	−2.05(10)	−14.84(4)	−13.74(7)	−1.10(8)
$E_{{}^{6}_{\Lambda\Lambda}{\rm He}} = E_\Lambda + E_{\rm NC}$	−35.07(5)	−34.32(2)	−0.75(5)	−35.36(5)	−34.51(2)	−0.85(5)	−35.67(5)	−34.75(3)	−0.92(6)
$B_{\Lambda\Lambda}$	7.34(5)	6.60(4)	0.74(6)	7.63(5)	6.78(4)	0.85(6)	7.94(5)	7.02(4)	0.92(6)
$\Delta B_{\Lambda\Lambda}$	1.13(6)	0.36(4)	0.77(7)	1.39(6)	0.54(4)	0.85(7)	1.70(6)	0.78(4)	0.92(7)

been noticed [14]. As a result, even the central quantities change with the variation of ε. The Nijmegen phase equivalent $\Lambda\Lambda$ potential $v_{\Lambda\Lambda}$ is found to decrease with decreasing ε. So also is the case with repulsive $V^D_{\lambda ij}$, which has a very weak spin dependence for the spin zero core nucleus, therefore it is almost a central term. Though not linearly, the $v_{\lambda i}$ too decreases with decreasing ε.

As mentioned in the previous section, strength W^D of $V^D_{\lambda ij}$ is adjusted to reproduce the $B^{\rm exp}_\Lambda$ of ${}^{5}_{\Lambda}$He because the binding energy of the hypernucleus is sensitive to ε, which at a fixed W^D increases with decreasing ε. Thus, a higher value of W^D is inevitably required to reproduce $B^{\rm exp}_\Lambda$ at lower ε. As a result, the expectation value of $V^D_{\lambda ij}$, which is a positive quantity, is higher at lower ε. Therefore, it resists any change in $v_{\Lambda i}$ and $v_{\Lambda\Lambda}$ with respect to the variation in ε. The $V^{2\pi}_{\lambda ij}$ is sensitive to operatorial correlations, especially the tensor correlation and to its self-induced correlation as it has a generalized tensor-τ type of operatorial structure. This has already been discussed in Ref. [14] and in references cited therein. To check this operatorial sensitivity of $V^{2\pi}_{\lambda ij}$, we perform independent calculations with $\overline{v}2$ and $\varepsilon = 0.2$ after switching off all the operatorial correlations in the WF. The $\langle V^{2\pi}_{\lambda ij}\rangle$ turns out to be $-1.04(1)$ MeV, whose value with full WF

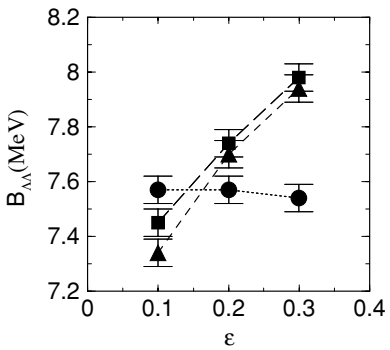

FIG. 2. $B_{\Lambda\Lambda}$ vs ε. Crcles, triangles, and squares represent $\overline{v}1$, $\overline{v}2$, and $\overline{v}3$, respectively.

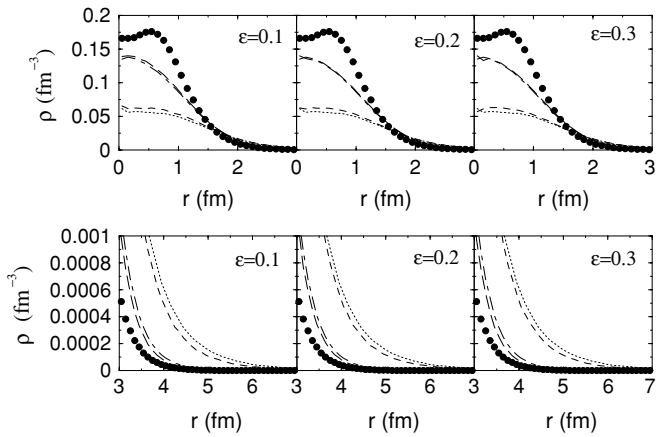

FIG. 3. Dotted and dashed lines represent Λ densities with and without SEC, respectively. Chain and long-dashed lines represent p densities with and without SEC, respectively. Filled circles show p in ^{4}He nucleus.

TABLE V. Nuclear core polarization (NCP). The ${}^{5}_{\Lambda}$He results are taken from Ref. [14].

	$\varepsilon = 0.1$				$\varepsilon = 0.2$				$\varepsilon = 0.3$			
	${}^{6}_{\Lambda\Lambda}$He		${}^{5}_{\Lambda}$He		${}^{6}_{\Lambda\Lambda}$He		${}^{5}_{\Lambda}$He		${}^{6}_{\Lambda\Lambda}$He		${}^{5}_{\Lambda}$He	
	(SEC) (MeV)	(No SEC) (MeV)	(SEC) (MeV)	(No SEC) (MeV)	(SEC) (MeV)	(No SEC) (MeV)	(SEC) (MeV)	(No SEC) (MeV)	(SEC) (MeV)	(No SEC) (MeV)	(SEC) (MeV)	(No SEC) (MeV)
$\overline{v}1$	8.39(6)	8.86(4)	3.59(4)	4.31(3)	7.83(6)	8.86(4)	3.16(4)	4.31(3)	7.57(6)	8.86(4)	2.70(4)	4.31(3)
$\overline{v}2$	9.20(6)	7.57(4)	2.93(4)	3.22(4)	9.18(6)	10.36(4)	2.61(4)	3.22(4)	8.80(6)	11.50(4)	2.39(4)	3.22(4)
$\overline{v}3$	8.86(6)	8.29(4)	2.19(4)	2.39(4)	9.45(6)	12.46(4)	1.91(4)	2.39(4)	11.07(6)	12.21(4)	1.69(4)	2.39(4)

is $-6.01(2)$ MeV. There it shows a strong effect of operators. The density effect also enters through $Y_\pi(r)$ and $T_\pi(r)$ radial functions. It offsets the tuning of the wave function and hence affects the complete energy breakdown. Though this quantity is attractive, it increases with decreasing ε and has the same trend as $V^D_{\lambda ij}$. The nuclear core energy, $E_{\rm NC} = T_i + v_{ij} + V_{ijk}$, too increases with decreasing ε. Hence, it falls in line with $V^D_{\lambda ij}$ and $V^{2\pi}_{\lambda ij}$. Therefore, both the quantities $V_{\lambda ij} = V^D_{\lambda ij} + V^{2\pi}_{\lambda ij}$ and $E_{\rm NC}$ together oppose $v_{\Lambda i}$ and $v_{\Lambda\Lambda}$ against any change in ε.

The constant binding energy of the hypernucleus both with and without SEC for $\overline{v}1$ with respect to variation in ε is almost an accident, because a change in $v_{\lambda i}$ and $v_{\Lambda\Lambda}$ due to it is balanced by an opposite effect in $V_{\lambda ij}$ and $E_{\rm NC}$. However, at lower $\overline{v}$ like $\overline{v}2$ and $\overline{v}3$, the changes in $V_{\lambda ij}$ and $E_{\rm NC}$ win over the changes in $v_{\lambda i}$ and $v_{\Lambda\Lambda}$. Therefore, the total energy decreases with increasing ε($B_{\Lambda\Lambda}$ increases with increasing ε). Variation of $B_{\Lambda\Lambda}$ with respect to ε is quite linear within the limits of uncertainties. It may be expressed as $\partial B_{\Lambda\Lambda}/\partial\varepsilon = -\partial E_{{}^{6}_{\Lambda\Lambda}\rm He}/\partial\varepsilon \approx$ constant. In the case of ${}^{5}_{\Lambda}$He, a couple of linear relationships have been observed [14]. Those are (i) $\partial B_\Lambda/\partial\varepsilon \approx$ constant and (ii) $\partial V^D_{\Lambda ij}/\partial W^D = \partial E_{{}^{5}_{\Lambda}\rm He}/\partial W^D = -\partial B_\Lambda/\partial W^D \approx$ constant. This leads to another linear relationship $\partial W^D/\partial\varepsilon \approx -0.016(1)$ MeV. Therefore, with decreasing ε, strength W^D is increased appropriately so that it reproduces $B^{\rm exp}_\Lambda$ as mentioned in Sec. III. Hence, for every set of $\overline{v}$, $\partial B_\Lambda/\partial\varepsilon$ is balanced by $-\partial B_\Lambda/\partial W^D$. Therefore, total energy remains constant. However, the same strengths do not yield a constant energy for ${}^{6}_{\Lambda\Lambda}$He, except for $\overline{v}1$. As for $\overline{v}1$, $B_{\Lambda\Lambda}$ remains constant with the variation in ε. However, $B_{\Lambda\Lambda}$ increases linearly for $\overline{v}2$ and $\overline{v}3$ as shown in Fig. 2. Thus, like ${}^{5}_{\Lambda}$He, similar relationships are observed for ${}^{6}_{\Lambda\Lambda}$He. These are (i) $\partial B_{\Lambda\Lambda}/\partial\varepsilon = c_1$ at a fixed $\overline{v}$, and (ii) $\partial V^D_{\Lambda ij}/\partial W^D = -\partial E_{{}^{6}_{\Lambda\Lambda}\rm He}/\partial W^D = \partial B_{\Lambda\Lambda}/\partial W^D = c_2$. (Here, c_1 and c_2 are positive constants.) As a consequence, a linear relationship between ε and W^D is observed: $\partial W^D/\partial\varepsilon \approx c_3$. For ${}^{5}_{\Lambda}$He, the slope $c_3 \approx -0.016(1)$ MeV is observed [14]. However, for ${}^{6}_{\Lambda\Lambda}$He, the slope is different and depends upon $\overline{v}$. One of the reasons for this difference is the stronger SEC effect in the case of ${}^{6}_{\Lambda\Lambda}$He because of the presence of two Λ baryons, which also contribute to the incremental energy $\Delta B_{\Lambda\Lambda} = B_{\Lambda\Lambda} - 2B_\Lambda$.

For every set of strengths used herein, $B_{\Lambda\Lambda}$ falls in the range of 7.33(5) to 7.98(5) MeV. Here, we also notice that all three choices of $\overline{v}$ give almost the same energy (within the limits of statistical uncertainties) of the hypernucleus for a particular value of $\varepsilon \approx 0.16(2)$ as seen in Fig. 2. Therefore, $B_{\Lambda\Lambda}$ at this value of ε is invariant of $\overline{v}$, which is found to be about 7.57(5) MeV. In other words, a particular set of two- and three-body potential strengths that reproduces $B^{\rm exp}_\Lambda$ of ${}^{5}_{\Lambda}$He also gives a value quite close to the experimental $\Lambda\Lambda$-separation energy for ${}^{6}_{\Lambda\Lambda}$He, that is, $B^{\rm exp}_{\Lambda\Lambda} = 7.25(19)$ MeV. The small difference between theoretical and experimental values may well be removed through a small variation in γ used in $v_{\Lambda\Lambda}$. This strengthens confidence in the fully correlated WF including SEC. It also gives us hope for the resolution of the $A = 5$ anomaly [26,31,32].

We notice a large polarization of nuclear core for both choices of the WF, with and without SEC, as reported in Table V. These values are more than double those of ${}^{5}_{\Lambda}$He. In the case of ${}^{5}_{\Lambda}$He, NCP is found to significantly decrease with increasing ε. However, for ${}^{6}_{\Lambda\Lambda}$He, it varies slowly, perhaps

TABLE VI. Point proton radius of nuclear core (NC). The ${}^{5}_{\Lambda}$He results are taken from Ref. [14]. The uncertainties in the values are 0.001 and 0.002 for ${}^{5}_{\Lambda}$He and ${}^{6}_{\Lambda\Lambda}$He, respectively.

	$\varepsilon = 0.1$				$\varepsilon = 0.2$				$\varepsilon = 0.3$			
	${}^{6}_{\Lambda\Lambda}$He		${}^{5}_{\Lambda}$He		${}^{6}_{\Lambda\Lambda}$He		${}^{5}_{\Lambda}$He		${}^{6}_{\Lambda\Lambda}$He		${}^{5}_{\Lambda}$He	
	(SEC) (fm)	(No SEC) (fm)	(SEC) (fm)	(No SEC) (fm)	(SEC) (fm)	(No SEC) (fm)	(SEC) (fm)	(No SEC) (fm)	(SEC) (fm)	(No SEC) (fm)	(SEC) (fm)	(No SEC) (fm)
$\overline{v}1$	1.666	1.703	1.588	1.619	1.678	1.703	1.585	1.619	1.669	1.703	1.586	1.619
$\overline{v}2$	1.667	1.756	1.605	1.647	1.662	1.740	1.602	1.647	1.650	1.740	1.600	1.647
$\overline{v}3$	1.661	1.785	1.624	1.676	1.653	1.766	1.621	1.676	1.618	1.740	1.620	1.676

because the point proton radius of NC does not change to any significant value with the variation of ε (see Table VI). Thus, at a higher value of ε, the difference of NCP between ${}^{5}_{\Lambda}$He and ${}^{6}_{\Lambda\Lambda}$He is quite large. It also has a trend of increment with decreasing $\overline{v}$ in the case of ${}^{6}_{\Lambda\Lambda}$He. However, this effect is opposite in the case of ${}^{5}_{\Lambda}$He.

The point proton radius of NC without SEC is found to be more than 1.70 fm. However, with SEC, it reduces to about 1.65 fm. In the case of isolated ^{4}He, it is 1.46(1) fm, whereas the experimental value is 1.47 fm, which has been obtained by subtracting a proton mean square radius of 0.743 fm^2 and N/Z times a neutron mean square radius of -0.116 fm^2 from the square of the measured charge radius. Thus, NC gets compressed with SEC and becomes more compact. We may understand these results with the help of Figs 1 and 3. In Fig. 3, we plot the density profiles only for $\overline{v}1$, as the features are similar for $\overline{v}2$ and $\overline{v}3$. The repulsive correlation $f^c_{\Lambda N}$ pushes both the nucleons and the Λ toward the periphery and at the center of the hypernucleus. Similar effect is seen in the case of ${}^{17}_{\Lambda}$O [33] and of ${}^{5}_{\Lambda}$He [34,35]. As in Fig. 1, SEC significantly reduces the repulsive correlation in the interior region of the hypernucleus in the range $r \approx 0.5$–2.0 fm, thereby reducing the outward push. As a result, both nucleons and Λ receive an inward pull leading to reduction in the peripheral density profiles and enhancement in the interior density profiles (Fig. 3). Thus, both NC and the hypernucleus are found to be more compact with SEC. The result is similar for ${}^{5}_{\Lambda}$He, where a direct correlation between density profiles and reduction in the repulsive correlation $f^c_{\Lambda N}$ due to SEC is noticed as well [14]. However, features are more prominent in the case of ${}^{6}_{\Lambda\Lambda}$He. This is certainly because of the presence of two Λ hyperons.

V. CONCLUSION

Conclusively we observe that SEC, being an important correlation, strongly affects energy breakdown, $\Lambda\Lambda$-separation energy, nuclear core polarization, point proton radius, and density profiles. All these physical observables are found to be sensitive to ε when SEC is invoked in the WF. Similar results are obtained for ${}^{5}_{\Lambda}$He as in Ref. [14]. The present investigation confirms the conclusions drawn therein. Comparison of the results of ${}^{5}_{\Lambda}$He and ${}^{6}_{\Lambda\Lambda}$He demonstrates that SEC effects are more evident with the increasing quantum of strangeness. We observe that the strengths that reproduce experimental Λ-separation energy of ${}^{5}_{\Lambda}$He also yield a result quite close to the experimental $\Lambda\Lambda$-separation energy of ${}^{6}_{\Lambda\Lambda}$He with the phase equivalent Nijmegen ND model $\Lambda\Lambda$ potential. Though $B_{\Lambda\Lambda}$ so obtained varies with ε and also with the choice of $\overline{v}$; it remains almost constant to a value quite close to the experimental value at $\epsilon \approx 0.16(2)$. Thus, a slight variation in γ would reproduce $B^{\rm exp}_{\Lambda\Lambda}$ of ${}^{6}_{\Lambda\Lambda}$He and also $B^{\rm exp}_{\Lambda}$ of ${}^{5}_{\Lambda}$He with the use of same two- and three-body potential strengths. The value of γ used in the phenomenological $\Lambda\Lambda$ potential would be slightly smaller with SEC in the WF than in the no SEC case. The s-wave ΛNN potential though small is not a negligible quantity. The polarization of the NC is large. The nucleon and Λ density profiles are affected by SEC, especially in the peripheral region, where Λ skin is also observed. The hypernucleus and its NC are found compact with SEC.

The outcome of the investigation presented herein thus suggests that (i) a study ignoring SEC in the WF would be deficient, (ii) a similar study for all the s-shell double hypernuclei is needed, and (iii) the behavior of $\Lambda\Lambda$-separation energy vis-a-vis potential strengths should be thoroughly investigated. A detailed comparison of the various phenomenological $\Lambda\Lambda$ potentials would also be interesting. We aim to proceed in this direction.

ACKNOWLEDGMENTS

The work was supported under Grant No. SP/S2/K-32/99 awarded to A.A.U. by the Department of Science and Technology, Government of India. Z.H. acknowledges support through a University Junior Research Fellowship.

[1] H. Takahashi *et al.*, Phys. Rev. Lett. **87**, 212502 (2001).
[2] J. K. Ahn *et al.*, Phys. Rev. Lett. **87**, 132504 (2001).
[3] M. Danysz *et al.*, Nucl. Phys. **49**, 121 (1963); Phys. Rev. Lett. **11**, 29 (1963).
[4] R. H. Dalitz, D. H. Davis, P. H. Fowler, A. Montwill, J. Pneiswki, and J. A. Zakrzewski, Proc. R. Soc. London, Ser. A **426**, 1 (1989).
[5] S. Aoki *et al.*, Prog. Theor. Phys. **85**, 1287 (1991).
[6] C. B. Dover, D. J. Millener, A. Gal, and D. H. Davis, Phys. Rev. C **44**, 1905 (1991).
[7] I. N. Filikhin and A. Gal, Nucl. Phys. **A707**, 491 (2002).
[8] I. N. Filikhin and A. Gal, Phys. Rev. C **65**, 041001(R) (2002).
[9] I. N. Filikhin and A. Gal, Phys. Rev. Lett. **89**, 172502 (2002).
[10] I. N. Filikhin, A. Gal, and V. M. Suslov, Phys. Rev. C **68**, 024002 (2003).
[11] E. Hiyama, M. Kamimura, T. Motoba, T. Yamada, and Y. Yamamoto, Phys. Rev. C **66**, 024007 (2002).
[12] M. Shoeb, Phys. Rev. C **69**, 054003 (2004).
[13] Q. N. Usmani, A. R. Bodmer, and B. Sharma, Phys. Rev. C **70**, 061001(R) (2004).
[14] A. A. Usmani, Phys. Rev. C **73**, 011302(R) (2006).
[15] A. Nogga, H. Kamada, and W. Glockle, Phys. Rev. Lett. **88**, 172501 (2002).
[16] H. Nemura, Y. Akaishi, and Y. Suzuki, Phys. Rev. Lett. **89**, 142504 (2002).
[17] Th. A. Rijken, V. G. J. Stoks, and Y. Yamamoto, Phys. Rev. C **59**, 21 (1999).
[18] E. Hiyama, M. Kamimura, T. Motoba, I. Yamada, and I. Yamamoto, Prog. Theor. Phys. **97**, 881 (1997).
[19] A. R. Bodmer, Q. N. Usmani, and J. Carlson, Phys. Rev. C **29**, 684 (1984).
[20] I. E. Lagaris and V. R. Pandharipande, Nucl. Phys. **A359**, 331 (1981).
[21] A. R. Bodmer and Q. N. Usmani, Nucl. Phys. **A477**, 621 (1988).
[22] R. B. Wiringa, V. G. J. Stoks, and R. Schiavilla, Phys. Rev. C **51**, 38 (1995).

[23] B. S. Pudliner, V. R. Pandharipande, J. Carlson, and R. B. Wiringa, Phys. Rev. Lett. **74**, 4396 (1995).
[24] J. Carlson, V. R. Pandharipande, and R. B. Wiringa, Nucl. Phys. **A401**, 59 (1983).
[25] R. K. Bhaduri, B. A. Loiseau, and Y. Nogami, Ann. Phys. (NY) **44**, 57 (1967).
[26] A. Gal, Adv. Nucl. Phys. **8**, 1 (1975).
[27] Q. N. Usmani and A. R. Bodmer, Phys. Rev. C **60**, 055215 (1999).
[28] A. R. Bodmer and D. M. Rote, Nucl. Phys. **A169**, 1 (1971).
[29] J. Rozynek and J. Dabrowski, Phys. Rev. C **20**, 1612 (1979); J. Dabrowski and J. Rozynek, *ibid*. **23**, 1706 (1981); Y. Yamamoto and H. Bando, Prog. Theor. Phys. **81**, 9 (1985); Y. Yamamoto, Nucl. Phys. **A450**, 275c (1986).
[30] A. R. Bodmer, D. M. Rote, and A. L. Mazza, Phys. Rev. C **2**, 1623 (1970).
[31] R. H. Dalitz, R. C. Herndon, and Y. C. Tang, Nucl. Phys. **B47**, 109 (1972).
[32] E. V. Hungerford and L. C. Biedenhorn, Phys. Lett. **B142**, 232 (1984).
[33] A. A. Usmani, S. C. Pieper, and Q. N. Usmani, Phys. Rev. C **51**, 2347 (1995).
[34] A. A. Usmani, Phys. Rev. C **52**, 1773 (1995).
[35] A. A. Usmani and S. Murtaza, Phys. Rev. C **68**, 024001 (2003).